Original scientific paper
https://doi.org/10.33180/InfMIDEM2024.304

Informacije MIDEM
Journal of Microelectronics,
Electronic Components and Materials
Vol. 54, No. 3(2024), 201 – 213

A Novel Method for 5Generation Multiple-Input, Multiple-Output Orthogonal Frequency-Division Multiplexing using Cauchy Evading Golden Tortoise Adaptive-Bi Directional-Long Short-Term Memory

Poornima Ramamoorthy[1], Kalaivani Ramanathan[2]*

[1]Department of Electronics and Communication Engineering, SNS College of Technology, Coimbatore, Tamil Nadu, India.
[2]Department of Electronics and Communication Engineering, Erode Sengunthar Engineering College, Perundurai, Tamil Nadu, India.

Abstract: Multiple-Input Multiple Output Orthogonal Frequency Division Multiplexing (MIMO-OFDM), which could provide a large number of antennas, is one among the key technologies of 5G. For recovering the transmitted symbols at the receiver, a key role is played by the Channel Estimation (CE) in MIMO-OFDM. But it is indisputable recently. Hence, a novel method for 5G MIMO-OFDM CE using Cauchy Evading Golden Tortoise Adaptive-Bi Directional-Long Short-Term Memory (CEGTA-Bi-LSTM) is proposed. Primarily, input like text, video, and audio are given for the encoding process at the transmitter; in addition, it is encoded using the Gaussian Distribution-Low Density Parity Check (GD-LDPC) algorithm. Then, by employing Combined Bits-Quadrature Phase Shift Keying (CB-QPSK), the signal is modulated. Next, the output is inputted into the pulse shaping, which is conducted by deploying Truncated Linear-Raised Cosine Filter (TL-RCF). The pulse-shaped signal is fed into the pilot insertion phase where the reference signal is inserted. Afterward, the signal is inputted into the Entropy-Inverse Fast Fourier Transform (E-IFFT) phase. Next, the output from the E-IFFT passes through the channel with AWGN noise; also, it is given to the receiver phase in which the reverse process of the transmitter occurs. Then, from the receiver output, the channel is estimated. The proposed CEGTA-Bi-LSTM is implemented using MATLAB simulation. The experimental results show that, the proposed method decrease the Mean Squared Error (MSE) by 0.7%, 1.6%, 2.6% lower than Bi-directional Long Short-Term Memory (Bi-LSTM), Long Short-Term Memory (LSTM), Least Squares (LS), and Minimum Mean Square Error (MMSE) respectively.

Keywords: MIMO-OFDM; 5G; Channel Estimation; transmitter

Nova optimizacijska metoda izogibanja zlati želvi za oceno MIMO OFDM 5G kanala

Izvleček: Več vhodni in več izhodni ortogonalni frekvenčni multiplekser (MIMO-OFDM), ki lahko zagotovi veliko število anten, je ena od ključnih tehnologij 5G. Za obnovitev poslanih simbolov v sprejemniku ima pri MIMO-OFDM ključno vlogo ocenjevanje kanala (CE). Predlagana je nova metoda za 5G MIMO-OFDM CE z uporabo izogibanja zlati želvi (CEGTA-Bi-LSTM). Vhodni podatki, kot so besedilo, video in zvok, so v prvi vrsti dani za postopek kodiranja na oddajniku; poleg tega se kodirajo z algoritmom Gaussian Distribution-Low Density Parity Check (GD-LDPC). Nato se signal modulira z uporabo kombiniranega bitno-kvadraturnega faznega premikanja ključev (CB-QPSK). Izhodni signal se vnese v oblikovanje impulzov, ki se izvede z uporabo skrajšanega linearnega dvignjenega kosinusnega filtra (TL-RCF). Impulzno oblikovani signal se vodi v fazo vstavljanja pilotnega signala, v katero se vstavi referenčni signal. Po entropijski obratni Fourierova transformaciji (E-IFFT), preide signal skozi kanal s šumom AWGN; prav tako se posreduje v fazo sprejemnika, v kateri se izvede obraten postopek kot pri oddajniku. Nato se na podlagi izhoda sprejemnika oceni kanal. Eksperimentalni rezultati kažejo, da predlagana metoda zmanjša srednjo kvadratno napako (MSE) za 0,7 %, 1,6 % in 2,6 % v primerjavi z dvosmernim dolgotrajnim spominom (Bi-LSTM), dolgotrajnim spominom (LSTM), najmanjšo kvadratno napako (LS) in najmanjšo srednjo kvadratno napako (MMSE).

Ključne besede: MIMO-OFDM; 5G; ocenjevanje kanala; oddajnik

** Corresponding Author's e-mail: poornima7654@outlook.com*

How to cite:
P. Ramamoorthy et al., "A Novel Method for 5Generation Multiple-Input, Multiple-Output Orthogonal Frequency-Division Multiplexing using Cauchy Evading Golden Tortoise Adaptive-Bi Directional-Long Short-Term Memory", Inf. Midem-J. Microelectron. Electron. Compon. Mater., Vol. 54, No. 3(2024), pp. 201–213

1 Introduction

An antenna technology, which includes a huge number of antennas at the Base Station (BS), for serving various User Terminals (UTs) is termed a MIMO [1]. Users can be served by MIMO in the same time-frequency resources; hence, (A) spectrum efficiency, (B) energy efficiency, (C) spatial resolution, along with (D) network coverage can be enhanced. For the 5G and future wireless communication networks, it is considered as an optimistic technique owing to its merits [2]. High Spectral Efficiency (SE), high data rate, and low latency are encompassed in5G networks; in addition, they could connect more different devices, make businesses and industries more efficient and give consumers access to more information faster than ever before [3]. Besides, Wireless network suffers from certain challenges, namely frequency-selective fading, and dispersion. Dynamic tolerance of fading and dispersion is the key reason behind OFDM [4, 5]. In next-generation wireless communication systems, for tackling the ever-growing demands for higher SE, fusing massive MIMO with OFDM is a solution [6]. CE is required to obtain the signal transmission exactly in MIMO-OFDM. In wireless systems, CE is a challenging problem owing to the noise effect and time-varying of wireless channels [7]. Thus, the '2' CE methodologies like pilot tone-centric CE approach and blind or semi-blind CE are wielded to deal with this [8]. For acquiring the minimal mean square error, the pilot sequence and tones were optimized in the pilot tone estimation system; in addition, the system's estimation accuracy is liable to noise along with inter-carrier interference [9]. In the target cell, data of different users are sequentially detected by the blind or Semi-blind estimator along with formulates a constrained minimization issue for each user [10]. Some of the conventional approaches based on neural networks are fairly complex; also, require a large number of parameters to be trained with large datasets in DL [11]. Moreover, a lot of computational resources are required by a few machines learning-based algorithms. For estimating the relevant channel state, these approaches are not perfect. Thus, this paper proposes a new method for 5g MIMO-OFDM CE using the CEGTA-Bi-LSTM framework.

1.1 Problem statement

For solving the problem of CE, prevailing research methodologies have many ideas but still improvements are needed. Existing research methodologies have some drawbacks, which are described as follows,

- Least Squares (LS) estimation has comparatively higher estimation error owing to its low cost devoid of any prior statistical information concerning the channel, although it is hugely deployed for acquiring channel estimates.
- During ISI mitigation, the cyclic prefix's usage to avoid Inter Symbol Interference (ISI) introduces a loss in the SNR of the received signal.
- Most of the baseline CE techniques use QAM for signal modulation. However, the disadvantages of such a technique are that it is more prehensile to noise. Due to this QAM, the receiver is more difficult compared to receivers of other modulations for the process of secure transmission.
- CE models used in existing frameworks require prior knowledge of channel statistics. This makes the optimal channel predictor highly complex.

1.2 Objectives

In the existing CE model, the aforementioned loopholes can be overcome by proposing a novel method for 5G MIMO-OFDM CE using the CEGTA-Bi-LSTM framework. The research objectives of the proposed framework are listed as follows,

- For secure transmission between multipath channels, a GD-LDPC encoding model is introduced to encode the input.
- To propose a CB-QPSK modulation method for reducing the SER.
- A TL-RCF is utilized to alleviate ISI and prevents information loss.
- To model a novel DL-based CE technique by considering statistical channel properties with low estimation error using CEGTA-Bi-LSTM.

The remaining part is arranged as: the related works to the proposed methodology are elucidated in section 2; the proposed research methodology is delineated as in section 3; the experimental perusal is exhibited in section 4; the paper is winded up with the future work in section 5.

2 Related work

In 2021, Mashhadi & Gunduz, [12] recommended a neural network (NN)-centric joint pilot design and downlink CE system for Frequency Division Duplex (FDD) MIMO-OFDM systems. For frequency-aware pilot design, fully connected layers were deployed. By assigning pilots across subcarriers non-uniformly, the pilot overhead was effectively minimized. Channel statistics were required by the deployed CE. It made the presented method highly complicated.

In 2019, Kansal et al., [13] presented an innovative solution, which fuses OFDMA technologies with multi-user massive MIMO technology. Source encoding, channel encoding, interleaving, and modulation were included here. The highest SE was offered by the technique.

When weighed against the Fast Fourier Transform (FFT), this system grounded on the fractional Fourier transform (FRFT) provides lower SNR of 8–13 dB.

In 2019, Mehrabi et al., [14] developed a fresh DL-centric Decision-Directed-CE (DD-CE) for tracking fading channels and detecting data for longer packets even in fast vehicular environments and studied DD-CE systems. This technique profited from an easy receiver design, which didn't depend on the fading channel's precise statistical model. The requirement for Doppler rate estimation was removed by the system's ability, which was challenging for highly dynamic vehicular environments.

In 2022, et al., [15] recommended a fresh sort of pilot sequences with diverse modulation orders to enhance spectrum efficiency. In MIMO-OFDM systems, the developed variable pilot-assisted CE was espoused with lower along with higher-order modulations. As per the simulation outcomes, for MIMO-OFDM systems' BER performance, this technique had 1–2 dB SNR gains. This system's CE was verified just in a single field; thus, unreliable CE might be offered.

In 2021, Cheng et al., [16] presented a combined time-variant Carrier Frequency Offset (CFO) along with frequency-selective channel response estimation for MIMO-OFDM for mobile users. The MIMO-OFDM's signal model was presented; in addition, as per the maximal likelihood criterion, the joint estimator was derived. When analogized to the grid search-centric technique, this system had lower computational complexity. However, it was deployed at higher mobile speeds.

In 2020, Mata & Boonsrimuang, 2020 [17] developed an effectual CE technique for a massive MIMO–OFDM system. The discrete Fourier transform estimator (DFE), which appraised the MIMO channels accurately, was deployed. It had elevated estimation accuracy along with superior BER with lower-complexity MIMO data detection. A lower transmission data rate of 32.5 Mbps was acquired.

In 2020, SURIAVEL RAO & Malathi, [18] explored a cyclic prefix-centric estimation system for carrier frequency offset, which was estimated in fusion with an actual evolutionary Cuckoo Search technique centered on the received carrier phase angle together with cyclic prefix information for efficient optimization. As per the outcomes, noise estimation along with compensation was enhanced. But, for facilitating the system's self-learning ability, this system had complex computations.

In 2021, Gao et al., [19] constructed an uplink transmission scheme in crowded linked cell-free massive MIMO-OFDM with fewer orthogonal pilots. For detecting active User Equipment (UEs), pilot phase shift hopping patterns were wielded for the pilot transmission. In median and 95%-likely performance, the minimal SE was enhanced among active UEs. But it was not reliable since it was apt just for crowded cell-free massive MIMO-OFDM systems.

In 2021, Riadi et al., [20] developed a least squares CE (LSCE) in the Uplink transmission for Massive MIMO in 5G wireless communications merged with Orthogonal Frequency Division Multiplexing together with higher-order M-ary quadrature amplitude modulation (M-QAM) modulation. As per the simulation outcomes, the MMSE along with Zero-Forcing (ZF) detectors' performance was just less than 1 dB. Several antennas were deployed; thus, various RF modules were caused.

In 2022, Jothi & Chandrasekar, [21] introduced a MIMO-OFDM multimedia model with very low power consumption, which offered superior energy-efficacy. For delivering augmented QoS, the MIMO methodology was fused into an OFDM for multimedia wireless communication. The system's superiority lies in the 40% augmentation of processing time along with the 94% enhancement in energy efficiency at 25W in the 35th iteration. This system was not feasible since the system acquired low outcomes.

3 Proposed channel estimation using CEGTA-BI-LSTM in 5G

Owing to the DL's better potential, it has been employed for CE. Nevertheless, it is indisputable that the foundation of the overall network-level performance is

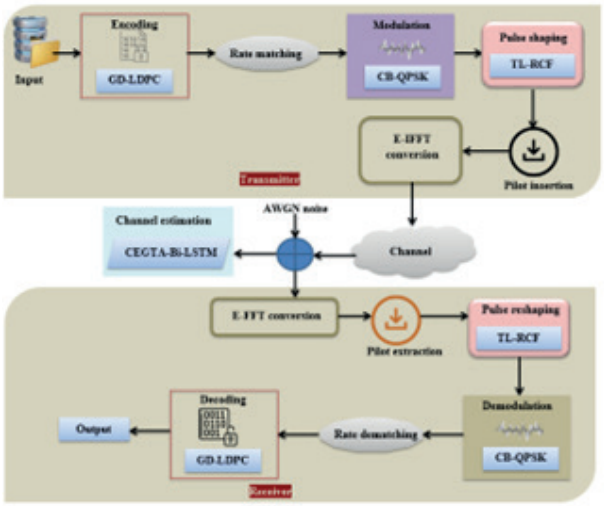

Figure 1: Proposed architecture for the channel estimation in 5G.

set by the processing employed in the physical layer. Hence, this paper proposes a new technique of MIMO-OFDM CE using CEGTA-Bi-LSTM in 5G wireless communication. In Figure 1, the proposed methodology's block diagram is depicted.

3.1 Transmitter

Here, the input file is given as input. Next, in the transmission process, the encoding, rate matching, modulation, Pulse shaping, Pilot insertion, and E-IFFT conversion occurs.

3.1.1 Input

Primarily, the input files from public resources are inputted into the proposed structure. It is equated as,

$$\zeta = \left\{\zeta_1, \zeta_2, \zeta_3, ..., \zeta_b\right\} or \zeta_a, a = 1, 2, 3, ..., b \quad (1)$$

Here, the total number of inputs is signified as ζ_a and the input file with *b* number of inputs is depicted as *a*.

3.1.2 Encoding

The input (ζ_a) is given as a matrix form to the encoding phase. Here, by employing the GD-LDPC, the inputs are encoded. For transmitting the data securely, encoding is deployed. A large message block is divided into several code blocks with a length of the code block in the LDPC model. Zeros will be padded at the end of the message if the last block is less than the length. This makes the sparsity matrix more complex. Thus, the GD function, which calculates the distribution between each input message bit and appends 0's and 1's based on the distribution function, is deployed to overcome this drawback. Thus, the complexity of obtaining a sparse matrix is minimized; in addition, makes the encoding more reliable. Primarily, let the parity check matrix of input (ζ_a) be (ψ). The parity matrix (ψ) is equated as,

$$\psi = \begin{bmatrix} 1 & 0 & 1 & 1 & 0 \\ 1 & 1 & 0 & 0 & 1 \\ 0 & 1 & 1 & 0 & 1 \\ \vdots & \vdots & \vdots & \vdots & \vdots \\ 1 & 0 & 0 & 1 & 0 \end{bmatrix} \quad (2)$$

The Gaussian distribution (GD) for the parity matrix $(\Im)$ is equated as,

$$\Im_{\upsilon\times\omega} = \frac{1}{D}\exp\left(\frac{-(\psi-\mu_m)}{2\sigma_s^2}\right) \quad (3)$$

$$D = \sqrt{2\pi\sigma_s^2} \quad (4)$$

Here, the normalization constant is depicted as *D*, the mean is signified as μ_m, and the variance is delineated as σ_s. From the GD parity matrix $(\Im)$, the generator matrix (ξ) is given by,

$$\xi = \left|\upsilon : \omega\right| \quad (5)$$

Here, the input vector is signified as υ, and the parity vector of the parity matrix is depicted as ω. Hence, the GD-LDPC block is equated as,

$$\xi\Theta\psi^T = 0 \quad (6)$$

Here, the transpose of the parity check matrix is signified as ψ^T. ϖ implies the output of the encoding phase using GD-LDPC. The pseudo-code for the proposed GD-LDPC is shown below.

PSEUDO CODE FOR GD-LDPC:

Input: Input files (ζ_a)

Output: Encoded bits (ϖ)
Begin
Initialize input vector (υ), parity vector (ω), normalization constant (*D*), and maximum iteration (J_{max}0)
Evaluate target
Set iteration $J = 1$
While $(J \le J_{max}())$ **do**
Assume the parity check matrix (ψ)
Generate GD for the parity check matrix,
$\Im_{\upsilon\times\omega} = \frac{1}{D}\exp\left(\frac{-(\psi-\mu_m)}{2\sigma_s^2}\right)$
Compute generator matrix
Evaluate GD-LDPC block, $\xi\Theta\psi^T = 0$
Compute target
If$(t\arg et \neq reached)${
Set $J = J + 1$
} **Else** {
Terminate
} **End if**
End while
Return encoded bits (ϖ)
End

3.1.3 Rate Matching

In the process of encoding (ϖ), the completed bits are inputted into the rate-matching phase for the process of extracting the exact set of bits to be transmitted within a given transmission time interval. Here, by employing rate matching, the range of bits to be transferred is performed. The rate matching (R_m) is equated as,

$$R_m = R_C^{-1}.(\varpi + 4) \tag{7}$$

Here, the code rate is depicted R_C^{-1}, the number of bits is signified as *m*, along with the encoded bits are delineated as ϖ.

3.1.4 Modulation

Here, after rate matching, the exact set of bits (R_m) obtained is mapped with CB-QPSK by utilizing the modulation block. The message signals cannot be transmitted over long distances since they have a very low frequency. Hence, modulation is essential. QPSK has a higher information transmission rate over other modulation techniques regarding which the QPSK has less bandwidth. One complex symbol as two binary bits is signified as QPSK. Thus, the QPSK receiver is more complex. The separated bits at the bit splitter are combined to mitigate such complexity. Next, for generating a Quadrature phase shift component, those combined mapped bits are multiplied with the same carrier. Primarily, the signals ($R_m(k)$) concerning time (*k*) are equated as,

$$R_m(k) = \sqrt{\frac{2\phi}{\lambda}} \cos\left(2\pi\gamma_x k + \hbar_c\right), c = 1,2,3,4.... \tag{8}$$

$$\hbar_c = (2c-1)\frac{\pi}{4} \tag{9}$$

Here, the energy per symbol is signified as ϕ, the angles of bits are depicted as $\hbar_c$, the symbol duration is delineated as λ, and the frequency of the carrier (*x*) is mentioned as γ_x. Hence, the two-dimensional signals space with unit basis functions $\alpha_1(k)$ and $\alpha_2(k)$ are equated,

$$\alpha_1(k) = \sqrt{\frac{2}{\lambda}} \cos\left(2\pi\gamma_x k\right), 0 \le k \le \lambda \tag{10}$$

$$\alpha_2(k) = \sqrt{\frac{2}{\lambda}} \sin\left(2\pi\gamma_x k\right), 0 \le k \le \lambda \tag{11}$$

The combined bits (CB) $(\Re)$ in QPSK in the factorial form are expressed as,

$$\Re = \frac{c!}{l!(c-l)!} \tag{12}$$

$$l = \delta_{c1}(k)\alpha_1(k) + \delta_{c2}(k)\alpha_2(k) \tag{13}$$

$$\delta_{c1} = \sqrt{\phi}\cos\hbar_c \tag{14}$$

$$\delta_{c2} = \sqrt{\phi}\sin\hbar_c \tag{15}$$

Here, the combination of the QPSK signal is signified as *l*, the first signal is delineated as δ_{c1}, and the second signal is depicted as δ_{c2}. Thus, signal-space 4 points are encompassed in the signal constellation, which is given by,

$$\left(\pm\sqrt{\frac{\phi}{2}}, \pm\sqrt{\frac{\phi}{2}}\right) \tag{16}$$

Here, the total energy is equally split between the two carriers. Q_p implies the modulated QPSK's output.

3.1.5 Pulse Shaping

The phase shifting output (Q_p) is inputted into the pulse shaping phase, which is wielded to avoid Inter-Symbol-Interference (ISI). TL-RCF technique is deployed. Pulse-shaping filter employed for modelling the transmitted input suited for the communication channel by limiting the bandwidth of transmission is termed the RCF. By limiting the bandwidth during transmission, the ISI caused by the channel could be kept in control. Timing jitter is caused since the RCF suffers from the problem of in-band ripple and out-of-band attenuation. By using a Truncated Linear (TL) function, the above-said downside can be surpassed to map the range between 0 and 1. Primarily, by employing the TL function $(\aleph_\nu())$, the modulated output (Q_p) is truncated, which is equated as,

$$\aleph_\nu(Q_p) = \min\left(1, \max\left(0, \left(\frac{1+\nu}{2\nu}\right) + \frac{|Q_p|}{\nu}\right)\right) \tag{17}$$

Here, the roll-off area in the frequency domain is signified as ν. Next, a filter process is a performance by the truncated signal $(\aleph_\nu(Q_p))$ where the Raised Cosine (RC) filter $(\wp_r(j))$ is given by,

$$\wp_r(j)=\begin{cases}1, for\,|j|<2N_0-N\\ \cos^2\left[\frac{\pi}{4}\frac{|j|+N-2N_0}{N-N_0}\right], for\,2N_0-N<j<N\\ 0, for\,|j|>N\end{cases} \quad (18)$$

Here, the frequency is signified as *j*, the minimum Nyquist bandwidth is depicted as N_0, the transmission bandwidth depicted as *N*, surplus bandwidth is expounded as $N - N_0$, from this, signal Raised Cosine falls above bandwidth N_0 of the truncated signal $\left(\aleph_v\left(Q_p\right)\right)$ .The time domain $\left(\wp_r(k)\right)$ or impulse response of the RC filter is given by,

$$\wp_r(k)=\sin c\left(\frac{k}{V_0}\right)\left[\frac{\cos(2\pi\eta k)}{1-\left(2\eta k/V_0\right)^2}\right] \quad (19)$$

Here, the roll-of-factor is signified as η, and the bit interval is depicted as V_0.

3.1.6 Pilot Insertion

The filtered output $\left(\wp_r(k)\right)$ is inputted into the pilot insertion phase. Here, pilot signals, which are deployed as the reference signal for communication purposes, are inserted; in addition, it is utilized to avoid noise. The estimation of frequency response at the pilot position (ℓ) is given by

$$\ell=\left(\wp_r(k)\right)^{-1} f_{pi} \quad (20)$$

Here, the received pilot vector is signified as f_{pi}.

3.1.7 E-IFFT Conversion

Next, for transforming the input as of the frequency domain to the time domain, the input bit (ℓ) undergoes E-IFFT since it offers a simple way to modulate data onto orthogonal subcarriers. However, FFT is restricted to the range of input to be transformed. Thus, tapering functions, namely the Entropy model is defined to compensate for spectral leakage. Hence, the input bit is evaluated in the entropy model, which is given by,

$$F=\ell_1\log_s\left(\frac{1}{\ell_1}\right)+\ell_2\log_s\left(\frac{1}{\ell_2}\right)+..... \quad (21)$$

Next, compute the entropy model with IFFT, (*p*(*y*)) which is given by,

$$p(y)=\sum_{q=0}^{W-1}F(q)S_W^{qy} \quad (22)$$

$$S_W^{qy}=e^{2\pi iqy/W} \quad (23)$$

Here, the input signal with range (*q*) is depicted as *F*(*q*), the FFT length is signified as *W*, the periodicity factor is mentioned as S_W^{qy}, and the number of outputs is delineated as *y*.

3.1.8 Communication

The time domain signal (*p*(*y*)) pass through the OFDM channel; in addition, for mimicking the effect of many random processes that occur in nature, AWGN noise is added to the channel. The output of the channel (S_i) is given by,

$$S_i=p(y)+N_s, i=1,2,.....,n \quad (24)$$

Here, the noise is depicted as N_s, and the total number of outputs is signified as *n*.

3.2 Receiver

The receiver receives the input (S_i) from the transmitter. In the transmitter, the operations are inversely done on the receiver block. Fast Fourier transform, Pilot extraction, Pulse reshaping, Demodulation, Rate dematching, and Decoding are done to retrieve the input data at the receiver. Finally, the original message can be viewed by the user. Next, by employing the transmitter phase and receiver phase, the process of CE takes place.

3.3. Channel Estimation

The proposed CEGTA-Bi-LSTM made the CE. Bi-LSTM is a DL neural network having the sequence information in both forward and backward directions with proper sigmoid activation function known as Adaptive Piecewise Linear Unit (APLU). This function can approximate any continuous function on a compact set which overcomes the gradient vanishing problem and improves the performance of CE. Several iterations are caused due to the random initialization of weight values; in addition, makes the estimation not static. Hence, for optimizing the network parameters, the CEGTO is proposed, which improves the performance of CE. The female beetle changes its position during the movement towards the golden male beetle. Now, there is a possibility of trapping in the local optimal solution by the female beetles. Thus, the protective strategies' efficacy for deterring predators may degrade. To update the female beetle solution, the Cauchy mutation strategy is utilized to preserve the details and also to preserve

the beetles falling to the local solution. Moreover, to prevent the protective strategies, an evading mechanism is introduced. To enhance the search capability of the golden tortoises, the Cauchy mutation strategy is briefly illustrated. Initially, the proposed CEGTO model divides the original population into '2' subpopulations in the evading mechanism. Next, two leaders with competitive fitness scores but low position proximity are identified. In Figure 2, the structure for the CEGTA-Bi-LSTM is shown.

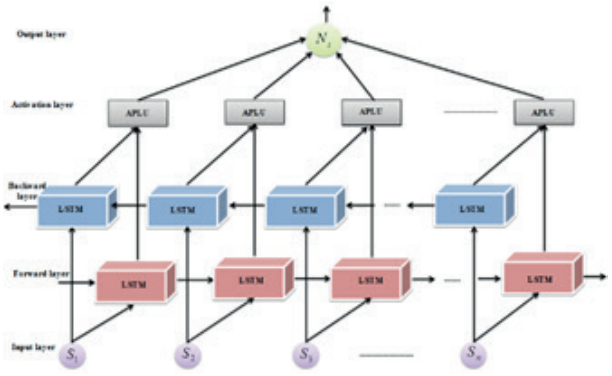

Figure 2: Architecture of the CEGTA-Bi-LSTM model.

Primarily, the received output (S_i) is inputted to the input layer of the proposed methodology. Next, initialize the weight values using the CEGTO [22] algorithm for the further process. The weight values are considered as golden tortoise beetles. Next, the initialized weight values are divided in to set of populations grounded on the best and worst velocity and position of the beetles using an evading process, which is given as follows,

$$\vartheta_{uL}^{v+1} = N * \vartheta_{uL}^{v} - d_1 * e_1 * \left(\varsigma_u - P_{uL}^{v}\right) - d_2 * e_2 * \left(\varepsilon - P_{uL}^{v}\right) \quad (25)$$

$$\varepsilon = \frac{z_1 + z_2 + z_3}{3} \quad (26)$$

$$P_{uL}^{v+1} = P_{uL}^{v} + \vartheta_{uL}^{v+1} \quad (27)$$

Here, the velocities of the u^{th} beetle during the v^{th} and $(v + 1)^{th}$ iteration of weight values are signified as ϑ_{uL}^{v+1} and ϑ_{uL}^{v}, the positions of the u^{th} beetle of weight values during the v^{th} and $(v + 1)^{th}$ iterations in the L^{th} dimension are depicted as P_{uL}^{v} and P_{uL}^{v+1}, the random vectors are signified as e_1 and e_2, the acceleration constants are mentioned as d_1 and d_2, the personal worst experience is expounded as ς_u, the mean solution of '3' global worst individuals is delineated as ε, and the iterations are depicted as z_1, z_2 and z_3. Moreover, the fitness of the two golden tortoises beetle group is computed. Accuracy is considered as fitness. For further process, the best velocity and best position beetles are utilized; in addition, low position proximity is also identified. In the u^{th} beetle, the x^{th} parameter's initial value $\left(\chi_{u,1}^{x}\right)$ at problem generation with L dimensions are given by,

$$\chi_{u,1}^{x} = \chi_{min}^{x_{max}^{u} x_{min}^{u}} \quad (28)$$

Here, the real-valued amounts uniformly distributed between the upper and lower bound of x^{th} parameter are depicted as χ_{min}^{x} and χ_{min}^{x}, and the lower bound parameter of the u^{th} beetle is mentioned as χ_{min}^{u}. Next, by employing '2' operators like the switching color operator along with the survival operator, the proposed system can be done.

a. Switching color operator

For mating with the golden beetle, the female beetle changes its position displaying an attractive golden color together with reproducing the next generation. Hence, the number of mature beetles' $\left(F_u^T\right)$ generated using the Cauchy mutation is given as,

$$F_u^T = B_u^T + Q_Z.\left(B_{gc_1}^T - \left(B_{best}^T + B_{best}^T.Cauchy\left(0,1\right)\right)\right) \quad (29)$$

$$Q_Z = \left(f_i g_i.\cos\left(\iota_i\right) + f_j g_j \cos\left(\iota_j\right)\right) + \left(t.\beta\right) \quad (30)$$

Here, the current female beetle's position in generation (T) is signified as B_u^T, which moves towards the golden male beetle $B_{gc_1}^T$ in generation (T) that has a golden color with a value determined by the color switching operator (Q_Z), a randomly generated integer is depicted as gc_1, the solution with the best fitness at the generation (T) is mentioned as B_{best}^T, the normal random functions of beetles are delineated as f_i, g_i, f_j, g_j, a random number is depicted as t, the wavelength is denoted as β, and the angles of beetles are depicted as ι_i and ι_j.

b) Survival Operator

In the eggs laid by the tortoise beetles, a few beetle eggs will survive owing to their protective strategies' efficacy in deterring predators. The survival operator is equated as,

$$\begin{cases} Bee_1 = \Omega\chi_1 + \left(1-\Omega\right).\left(\chi_1 - \sigma_1\right) \\ Bee_2 = \Omega\chi_2 + \left(1-\Omega\right).\left(\chi_2 - \sigma_2\right) \end{cases} \quad (31)$$

Where, the random number generator is signified as Ω, the randomly chosen solutions are depicted as χ_1 and

χ_2, and the variables are delineated as σ_1 and σ_2. (γ) implies the output of the CEGTO algorithm. It calculates the forward layer hidden sequence $\left(\vec{h}_p\right)$ and a backward layer hidden sequence $\left(\overleftarrow{h}_p\right)$ [23] from the opposite direction, which is given as follows,

$$\vec{h}_p = G\left(U_{\vec{h}\gamma}\gamma_n + U_{\vec{h}\vec{h}}\vec{h}_{n-1} + o_{\vec{h}}\right) \tag{32}$$

$$\overleftarrow{h}_p = G\left(U_{\overleftarrow{h}\gamma}\gamma_n + U_{\overleftarrow{h}\overleftarrow{h}}\overleftarrow{h}_{n-1} + o_{\overleftarrow{h}}\right) \tag{33}$$

Here, the forward input-hidden weight along with backward input-hidden weight matrices are depicted as $U_{\vec{h}\gamma}$ and $U_{\overleftarrow{h}\gamma}$, the previous forward and backward hidden sequence is signified as $\vec{h}_{n-1}$ and $\overleftarrow{h}_{n-1}$, the bias vectors in both directions are mentioned as $o_{\vec{h}}$ and $o_{\overleftarrow{h}}$, and the hidden layer is delineated as *G*. Hence, the encoded vector (g_w) is formed by the concatenation of the final forward layer and backward layer output with APLU activation function is given by,

$$g_w = W_f\left[\vec{h}_p, \overleftarrow{h}_p\right] \tag{34}$$

PSEUDO CODE FOR CEGTA-Bi-LSTM:

Input: Received output (S)
Output: Channel estimated output (N_s)
Begin
Initialize weight values, random number generator (Ω), and maximum iteration (P_{max} 0)
//Input layer
Initialize the weight values using CEGTO algorithm
Set iteration $P = 1$
While ($P \leq P_{max}$ 0) **do**
Perform Evading process,

$$\vartheta_{uL}^{v+1} = N * \vartheta_{uL}^{v} - d_1 * e_1 * \left(\varsigma_u - P_{uL}^{v}\right) - d_2 * e_2 * \left(\varepsilon - P_{uL}^{v}\right)$$

Evaluate fitness for both the population

If $\left(\boldsymbol{fitness \neq best}\right)${

Generate initial value
// switching color operator
Generate the number of mature beetles using Cauchy mutation,

$$F_u^T = B_u^T + Q_Z.\left(B_{gc_1}^T - \left(B_{best}^T + B_{best}^T.Cauchy(0,1)\right)\right)$$

//survival operator
Surviving of some beetles,

$$\begin{cases} Bee_1 = \Omega\chi_1 + (1-\Omega).(\chi_1 - \sigma_1) \\ Bee_2 = \Omega\chi_2 + (1-\Omega).(\chi_2 - \sigma_2) \end{cases}$$

} **Else** {

Set $\boldsymbol{P = P + 1}$

End if

End while
Return survived beetles (γ)

Perform forward layer hidden sequence $\left(\vec{h}_p\right)$

Perform backward layer hidden sequence $\left(\overleftarrow{\boldsymbol{h}}_{\boldsymbol{p}}\right)$
Evaluate output layer with APLU activation function,

$$g_w = W_f\left[U_{r\vec{h}}\vec{h}_p + U_{r\overleftarrow{h}}\overleftarrow{h}_p + o_r\right]$$

Return the channel estimated output
End

The above equation can also be written as,

$$g_w = W_f \left[U_{r\vec{h}} \vec{h}_p + U_{r\overleftarrow{h}} \overleftarrow{h}_p + o_r \right] \quad (35)$$

$$W_f = \mathrm{Re}\, Lu\left(h_p\right) + \sum_{e=1}^{l} F_e \max.\left(0, -h_p + H_e\right) \quad (36)$$

Here, the APLU activation function is depicted as W_f, the real numbers are signified as F_e and H_e, the total bias vectors are mentioned as o_r, the total of forward and backward layer hidden sequence is expounded as h_p, and the forward weight and backward weight matrices are embodied as $U_{r\vec{h}}$ and $U_{r\overleftarrow{h}}$. Hence, the output of the CE phase is given by,

$$N_s = S - p\left(y\right) \quad (37)$$

Here, the output of the channel estimator is depicted as N_s.The pseudo-code for the proposed CEGTA-Bi-LSTM is shown on the previous page.

By employing CEGTA-Bi-LSTM, the CE process is done. Thus, to prove the model's effectiveness, the evaluation of this proposed methodology is necessary. The result section is explained further.

4 Results and discussions

Here, a new technique of 5G MIMO-OFDM CE using CEGTA-Bi-LSTM is compared and analyzed. MATLAB is the working platform for this proposed methodology. From publicly available sources, the dataset is taken. Text, video, and audio are the '3' sorts of inputs.

4.1 Performance analysis

Grounded on '3' phases like encoding phase, modulation phase, and CE phase, the CE model is analyzed.

4.1.1 Performance analysis for encoding phase

Here, regarding encoding and decoding time, the proposed GD-LDPC's performance is weighed against the prevailing Low-Density Parity Check (LDPC), Huffman, Arithmetic, and Run Length.

The proposed GD-LDPCs are weighed against the prevailing methodologies in Table 1. The GD-LDPC acquired the lowest encoding and decoding time of 0.00575 s and 0.00131 s for text. For encoding and decoding, the GD-LDPC acquired 0.041 s and 0.0981 s for videos; while, the prevailing LDPC, Huffman, Arithmetic, and Run Length attained (0.0531 s and 0.0595 s), (0.0831 s and 0.0981 s), (1.0743 s and 0.1115 s), and (2.2401 s and 0.4472 s). The GD-LDPC also achieves the lowest time for audio. When analogized to other inputs, the proposed attains the lowest encoding and decoding time for text.

4.1.2 Performance analysis for modulation phase

Here, grounded on modulation and demodulation for the metrics Bit Error Rate (BER) and Peak Signal-to-Noise Ratio (PSNR), the proposed CB-QPSK's per-

Table 1: Performance analysis for the proposed GD-LDPC.

Algorithms	Text		Video		Audio	
	Encoding time (s)	Decoding time (s)	Encoding time (s)	Decoding time (s)	Encoding time (s)	Decoding time (s)
Proposed GD-LDPC	0.00575	0.00131	0.041	0.0498	0.04687	0.05571
LDPC	0.02507	0.01575	0.0531	0.0595	1.56224	0.0821
Huffman	0.08056	0.05668	0.0831	0.0981	1.71073	0.26549
Arithmetic	0.28189	0.55849	1.0743	0.1115	2.555	0.3
Run Length	0.92048	1.11424	2.2401	0.4472	7.22466	0.36

Table 2: Analysis of the proposed CB-QPSK with the existing algorithms.

Algorithms	Text		Video		Audio	
	BER (bits/sec)	PSNR (dB)	BER (bits/sec)	PSNR (dB)	BER (bits/sec)	PSNR (dB)
Proposed CB-QPSK	0.084058	58.00	0.09942	31.6	0.097	32.7
QPSK	0.120588	36.2	0.1542	26.1	0.12	26.9
PSK	0.144928	34.5	0.16415	23.9	0.155904	22.3
QAM	0.724638	33.9	0.17542	15.6	0.156827	16.2
FSK	1	17.7	0.354	10.6	1	10

formance is analogized to the prevailing Quadrature Phase Shift Keying (QPSK), Phase Shift Keying (PSK), Quadrature Amplitude Modulation (QAM), together with Frequency Shift Keying (FSK).

In Table 2, the performance analysis is depicted. The CB-QPSK attains the lowest BER. When analogized to the prevailing methodologies, the CB-QPSK achieves 58 dB for PSNR.

Likewise, for video, the CB-QPSK attains the lowest BER and higher PSNR. The CB-QPSK acquires the PSNR of 32.7 dB, which is 58 dB, 10.4 dB, 16.5 dB, and 22.7 dB lower when contrasted with the prevailing QPSK, PSK, QAM, and FSK; in addition, the CB-QPSK acquires lowest BER of 0.097 dB. Hence, enhanced outcomes are attained by the CB-QPSK.

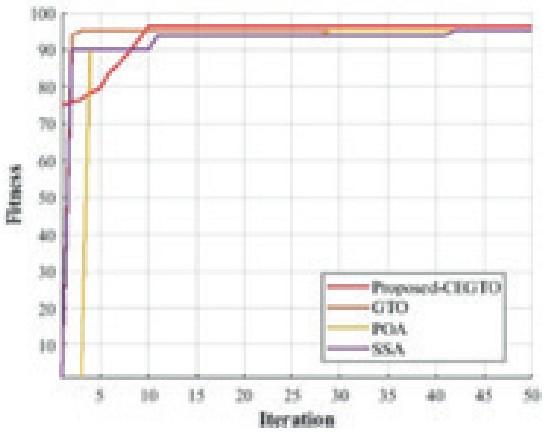

Figure 3: Fitness Vs iteration analysis.

4.1.3 Performance analysis for channel estimation
Here, grounded on PSNR, SE, Mean Squared Error (MSE), Symbol Error Rate (SER), and BER, the proposed CEGTA-Bi-LSTM's performance is analogized to the prevailing Bi-directional Long Short-Term Memory (Bi-LSTM), Long Short-Term Memory (LSTM), Least Squares (LS), and Minimum Mean Square Error (MMSE) centered on CE. In Figure 3, the fitness Vs iteration analysis for the proposed CEGTO is depicted.

4.1.3.1 Performance analysis for channel estimation
Here, regarding BER, MSE, PSNR, and SE, the CEGTA-Bi-LSTM's performance is weighed to the prevailing techniques.

In Figure 4, regarding (a) BER and (b) MSE, the CEGTA-Bi-LSTM's performance is analogized to the available methodologies. The proposed attains the BER and MSE values of 0.02 bits/sec and 3 at (5-10) SNR. The proposed algorithm attains the lowest BER and MSE values

(a)

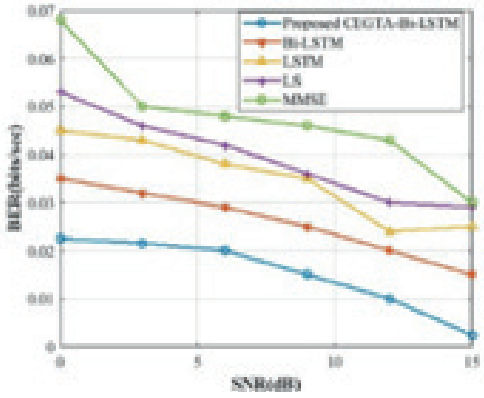

(b)

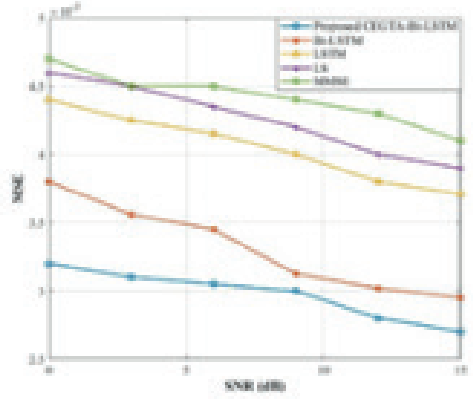

Figure 4: Performance analysis for the proposed algorithm with the existing algorithms based on (a) BER and (b) MSE.

at different SNR values. Hence, the CEGTA-Bi-LSTM is superior.

In Figure 5, regarding (a) PSNR, and (b) SE, the proposed CEGTA-Bi-LSTM's performance is evaluated with the available techniques. The CEGTA-Bi-LSTM attained the PSNR value approximately between 30dB and 35dB at (0-5) SNR; in addition, it acquired better results for the SE. The PSNR and SE values are better for all the SNR values.

4.1.3.2 Performance analysis for video data
Here, the CEGTA-Bi-LSTM's performance is evaluated with the prevailing systems grounded on BER, MSE, PSNR, and SE for video data.

The proposed technique is analyzed centered on (a) BER and (b) MSE in Figure 6. 0.05 to 0.1 at (10-15) SNR values; in addition, it attains enhanced outcomes for every SNR. Hence, the proposed system acquires superior outcomes for every metric.

In Figure 7, the proposed technique's performance is evaluated grounded on PSNR and SE. the proposed algorithm attains PSNR values approximately from 18

(a)

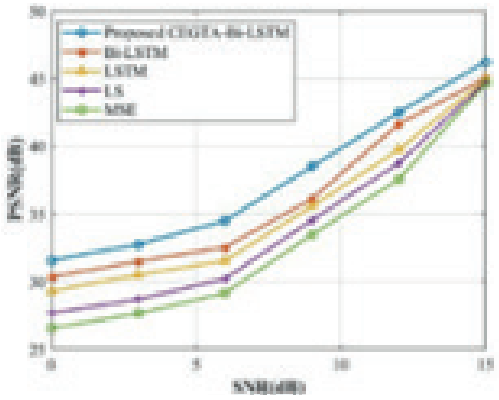

(b)

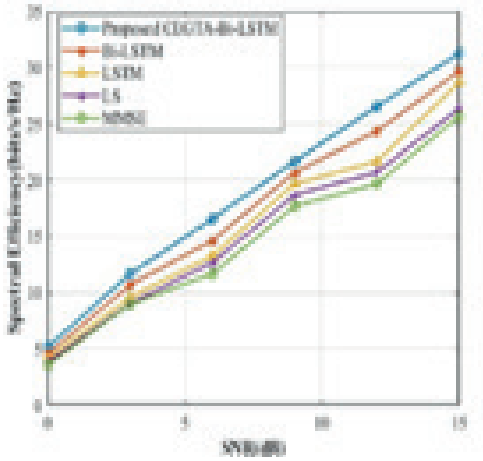

Figure 5: Graphical representation for the proposed algorithm with existing based on (a) PSNR and (b) SE.

to 26 dB at 0,5,10, and 15 SNRs, which is the highest PSNR value amongst the prevailing ones. The SE for the proposed algorithm is approximately 2 to 3 bits/s/Hz at 0dB SNR value. At every SNR value, the proposed algorithm performed better.

5 Conclusion

This paper proposes a new technique of 5G MIMO-OFDM CE by utilizing CEGTA-Bi-LSTM. The transmitter, channel, and receiver are encompassed in the proposed technique. The proposed methodology's performance metrics are compared and analyzed grounded on the inputs like text, video, and audio. The proposed GD-LDPC is compared with existing algorithms in the encoding phase and attains an encoding and decoding time of 0.00575 s and 0.00131 s for text. The proposed CB-QPSK is compared with the existing algorithms in the modulation phase and attained a lower PSNR of 31.564 dB for video. The proposed CEGTA-Bi-LSTM achieves a lower BER of 0.029684 bits/sec for audio in the CE phase. But this work considered only CE whereas the rate of data transmission and channel capacity of

(a)

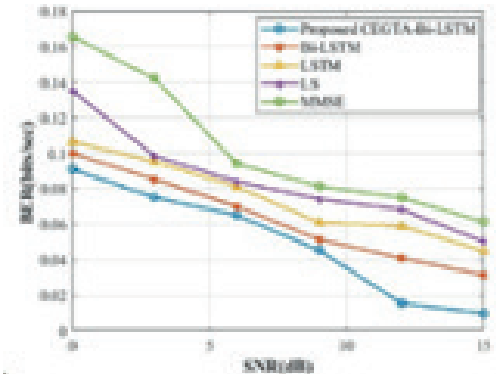

(b)

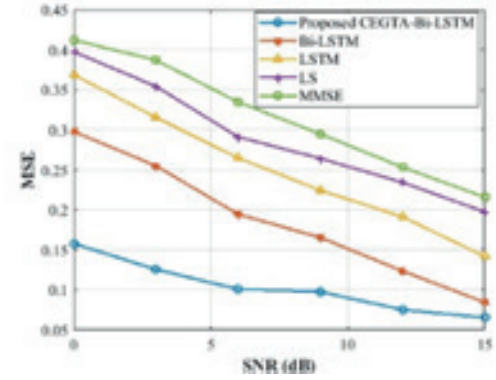

Figure 6: Performance analysis for the proposed with the existing based on (a) BER and (b) MSE.

(a)

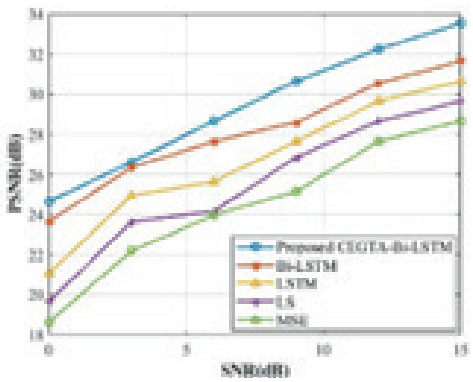

(b)

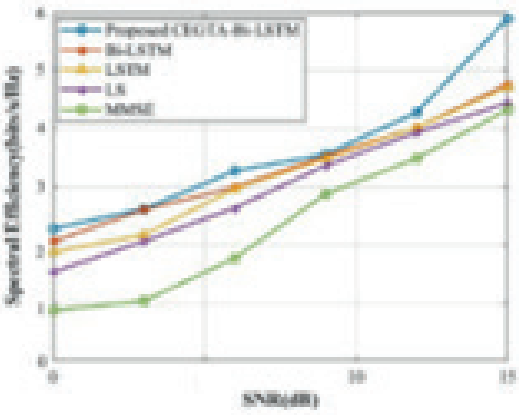

Figure 7: Graphical representation of (a) PSNR and (b) SE.

the system is not concentrated. In future, this work will be further enhanced by experimental implementation using LED and Optical Rx2 to improve transmission rate in channel estimation.

6 Acknowledgments

The author would like to express his heartfelt gratitude to Kalaivani Ramanathan the for her guidance and unwavering support during this research.

7 Conflict of Interest

The authors declare that they have no known competing financial interests or personal relationships that could have appeared to influence the work reported in this paper.

8 References

1. X. Liu, W. Wang, X. Song, X. Gao, G. Fettweis, "Sparse channel estimation via hierarchical hybrid message passing for massive MIMO-OFDM systems," IEEE Trans. Wireless Commun., 20, no. 11, pp. 7118–7134, 2021, https://doi.org/10.1109/TWC.2021.3080923
2. W. Ji, F. Zhang, L. Qiu, "Multipath Extraction Based UL/DL Channel Estimation for FDD Massive MIMO-OFDM Systems," IEEE Access, vol. 9, pp. 75349–75361, 2021, https://doi.org/10.1109/ACCESS.2021.3081497
3. R. Kanthavel, R. Dhaya and A. Ahilan, "AI-Based Efficient WUGS Network Channel Modeling and Clustered Cooperative Communication", *ACM Transactions on Sensor Networks*, vol. *18*, no. 3, 2022, http://dx.doi.org/10.1145/3469034
4. S. Nandi, N. N. Pathak, A. Nandi, "A Novel Adaptive Optimized Fast Blind Channel Estimation for Cyclic Prefix Assisted Space–Time Block Coded MIMO-OFDM Systems," Wireless Pers. Commun., vol. 115, no. 2, pp. 1317–1333, 2020. https://doi.org/10.1007/s11277-020-07629-z
5. Raghavendra, C.G., 2018. A novel approach to reduce the PMEPR of MCPC signal using random phase algorithm. *Informacije MIDEM*, *48*(1), pp.63-70.
6. E. Balevi, A. Doshi, J. G. Andrews, "Massive MIMO channel estimation with an untrained deep neural network," IEEE Trans. Wireless Commun., vol. 19, no. 3, pp. 2079–2090, 2020. https://doi.org/10.1109/TWC.2019.2962474
7. X. Cheng, R. Zayani, H. Shaiek, D. Roviras, "Inter-Numerology Interference Analysis and Cancellation for Massive MIMO-OFDM Downlink Systems," IEEE Access, vol. 7, pp. 177164–177176, 2019. https://doi.org/10.1109/ACCESS.2019.2957194
8. C. Venkateswarlu, N. V. Rao, "Optimal channel estimation and interference cancellation in MIMO-OFDM system using MN-based improved AMO model," J. Supercomput., vol. 78, no. 3, 3402–3424, 2022. https://doi.org/10.1007/s11227-021-03983-2
9. M. Prabhu, B. Muthu Kumar and A. Ahilan, "Slime mould algorithm based fuzzy linear CFO estimation in wireless sensor networks", *IETE Journal of Research*, pp. 1-11, 2023, https://doi.org/10.1080/03772063.2023.2194279
10. X. Hong, J. Gao, S. Chen, "Semi-blind joint channel estimation and data detection on sphere manifold for MIMO with high-order QAM signaling," J. Franklin Inst., vol. 357, no. 9, pp. 5680–5697, 2020. https://doi.org/10.1016/j.jfranklin.2020.04.009
11. P. Jiang, C. K. Wen, S. Jin, G. Y. Li, "Dual CNN-Based Channel Estimation for MIMO-OFDM Systems," IEEE Trans. Commun., vol. 69, no. 9, pp. 5859–5872, 2021. https://doi.org/10.1109/TCOMM.2021.3085895
12. M. B. Mashhadi, D. Gunduz, "Pruning the Pilots: Deep Learning-Based Pilot Design and Channel Estimation for MIMO-OFDM Systems," IEEE Trans. Commun., vol. 20, pp. 10, pp. 6315–6328, 2021, https://doi.org/10.1109/TWC.2021.3073309
13. L. Kansal, V. Sharma, J. Singh, "Multiuser Massive MIMO-OFDM System Incorporated with Diverse Transformation for 5G Applications," Wireless Personal Commun., vol. 109, no.4, pp. 2741–2756, 2019. https://doi.org/10.1007/s11277-019-06707-1
14. M. Mehrabi, M. Mohammadkarimi, M.Ardakani, Y. Jing, "Decision Directed Channel Estimation Based on Deep Neural Network k-Step Predictor for MIMO Communications in 5G," IEEE Journal on Selected Areas in Communications, vol. 37, no. 11, pp. 2443–2456, 2019. https://doi.org/10.1109/JSAC.2019.2934004
15. Q. Wu, X. Zhou, C. Wang, H. Cao, "Variable pilot assisted channel estimation in MIMO-OFDM system with STBC and different modulation modes," Eurasip Journal on Wireless Communications and Networking, 1-13, 2022, https://doi.org/10.1186/s13638-022-02126-2
16. N. H. Cheng, K. C. Huang, Y. F. Chen, S. M. Tseng, "Maximum likelihood-based adaptive iteration algorithm design for joint CFO and channel estimation in MIMO-OFDM systems," Eurasip Journal on Advances in Signal Processing, 1-21, 2021. https://doi.org/10.1186/s13634-020-00711-5
17. T. Mata, P. Boonsrimuang, "An Effective Channel Estimation for Massive MIMO–OFDM System,"

Wireless Personal Communications, vol. 114, no. 1, pp. 209–226, 2020. https://doi.org/10.1007/s11277-020-07359-2
18. R. S. Suriavel rao, P. Malathi, "A low complex cuckoo search optimizer based OFDM carrier frequency offset estimation for 5G wireless technology," International Journal of Dynamics and Control, vol. 7, no. 3, pp. 1125–1134, 2019, https://doi.org/10.1007/s40435-019-00526-9
19. J. Gao, Y. Wu, Y. Wang, W. Zhang, F. Wei, "Uplink transmission design for crowded correlated cell-free massive MIMO-OFDM systems," Science China Information Sciences, vol. 64, no. 8, pp. 1–16, 2021. https://doi.org/10.1007/s11432-020-3103-3
20. A. Riadi, M. Boulouird, M. M. Hassani, "ZF and MMSE Detectors Performances of a Massive MIMO System Combined with OFDM and M-QAM Modulation," Wireless Personal Communications, vol. 116, no. 4, pp. 3261–3276, 2021. https://doi.org/10.1007/s11277-020-07848-4
21. S. Jothi, A. Chandrasekar, "An Efficient Modified Dragonfly Optimization Based MIMO-OFDM for Enhancing QoS in Wireless Multimedia Communication," Wireless Personal Communications, vol. 122, no. 2, 1043–1065, 2022. https://doi.org/10.1007/s11277-021-08938-7
22. O. Tarkhaneh, N. Alipour, A. Chapnevis and H. Shen, 2021. "Golden tortoise beetle optimizer: a novel nature-inspired meta-heuristic algorithm for engineering problems", http://dx.doi.org/10.2139/ssrn.4538126
23. G. Parimala and R. Kayalvizhi, Automatic Intrusion Detection Using Optimal Features with Adaptive Bi-Directional Long Short Term Memory. International Journal of Intelligent Systems and Applications in Engineering, vol. 12, no. 4s, pp.710-716. 2024, http://dx.doi.org/10.1109/conit51480.2021.9498552

Copyright © 2024 by the Authors. This is an open access article distributed under the Creative Commons Attribution (CC BY) License (https://creativecommons.org/licenses/by/4.0/), which permits unrestricted use, distribution, and reproduction in any medium, provided the original work is properly cited.

Arrived: 25. 01. 2024
Accepted: 03. 07. 2024